Insulin Resistance, Brain Atrophy, and Cognitive Performance in Late Middle–Aged Adults

Auriel A. Willette, phd[1,2,3]
Guofan Xu, md, phd[1,3,4]
Sterling C. Johnson, phd[1,2,3]
Alex C. Birdsill, bs[1,3]
Erin M. Jonaitis, phd[3,5]

Mark A. Sager, md[3,5]
Bruce P. Hermann, phd[3,5]
Asenath La Rue, phd[3,5]
Sanjay Asthana, md[1,3,5]
Barbara B. Bendlin, phd[1,3]

OBJECTIVE—Insulin resistance dysregulates glucose uptake and other functions in brain areas affected by Alzheimer disease. Insulin resistance may play a role in Alzheimer disease etiopathogenesis. This longitudinal study examined whether insulin resistance among late middle–aged, cognitively healthy individuals was associated with 1) less gray matter in Alzheimer disease–sensitive brain regions and 2) worse cognitive performance.

RESEARCH DESIGN AND METHODS—Homeostasis model assessment of insulin resistance, gray matter volume, and the Rey Auditory Verbal Learning Test (RAVLT) were acquired in 372 participants at baseline and a consecutive subset of 121 individuals ~4 years later. Voxel-based morphometry and tensor-based morphometry were used, respectively, to test the association of insulin resistance with baseline brain volume and progressive gray matter atrophy.

RESULTS—Higher insulin resistance predicted less gray matter at baseline and 4 years later in medial temporal lobe, prefrontal cortices, precuneus, and other parietal gyri. A region-of-interest analysis, independent of the voxel-wise analyses, confirmed that higher insulin resistance was related to medial temporal lobe atrophy. Atrophy itself corresponded to cognitive deficits in the RAVLT. Temporal lobe atrophy that was predicted by higher insulin resistance significantly mediated worse RAVLT encoding performance.

CONCLUSIONS—These results suggest that insulin resistance in an asymptomatic, late middle–aged cohort is associated with progressive atrophy in regions affected by early Alzheimer disease. Insulin resistance may also affect the ability to encode episodic information by negatively influencing gray matter volume in medial temporal lobe.

Diabetes Care **36:443–449, 2013**

I nsulin signaling dysfunction adversely affects several neural processes, such as glucose uptake, and may precipitate brain atrophy in Alzheimer disease. People with Alzheimer disease often have higher insulin resistance (1), which reflects increased insulin levels and reduced binding efficacy on neuronal synapses and astrocytes (2). Insulin resistance may contribute to the etiopathogenesis of Alzheimer disease. Insulin resistance increases with age, poor diet, and lack of exercise, exerting adverse effects that may be distinctive from hyperglycemia in conditions such as type 2 diabetes (2,3). For instance, in the Rotterdam study, either a doubling of basal insulin levels or insulin resistance was associated with a 40%

increased likelihood of converting to Alzheimer disease at a 3-year follow-up from baseline (4). This relationship remained stable even after removal of participants with type 2 diabetes. In aged rhesus monkeys, a composite factor of insulin resistance and dyslipidemia was related to mitochondrial dysregulation in hippocampal regions (5). Conversely, long-term calorie restriction in older rhesus macaques raised insulin sensitivity, which predicted greater hippocampal volume; this relationship in turn mediated improved motor learning (6).

Insulin signaling normally facilitates microvascular blood flow, glucose uptake, and glucose oxidation for ATP generation (7). These effects predominantly occur in specific brain regions that have a high concentration of insulin receptors in rodents and are also affected by early Alzheimer disease, such as hippocampus, the prefrontal cortices, and cingulate gyrus (2,8,9). Insulin has other critical functions such as reducing accumulation and oligomerization of amyloid β (10,11), as well as reducing hyperphosphorylation of τ protein (12).

The effects of insulin resistance on brain volume are not well characterized. For regional gray matter volume, human studies have almost exclusively focused on the hippocampus. In a cross-sectional analysis of healthy later middle–aged to aged people, poor glucoregulation as assessed by a glucose tolerance test corresponded to lower hippocampal volume and poorer delayed recall on the Wechsler Paragraph test (3). Higher basal insulin resistance was also cross-sectionally associated with lower hippocampal volume and worse cognitive performance in healthy middle–aged women (13). In longitudinally assessed aged humans, higher fasting insulin showed small albeit significant correlations with gray matter atrophy in orbitofrontal cortex and hippocampus (14). Some groups, however, have not found this relationship between insulin resistance and hippocampus in late middle–aged (15) or geriatric (16) adults. Beyond the hippocampus, however, higher insulin reflective of insulin

- -

resistance does affect the cingulate cortices in early Alzheimer disease, although the relationship is paradoxically beneficial (17). We similarly found that lower insulin sensitivity predicted higher anterior cingulate gray matter in aged rhesus macaques fed an enriched, nonrestricted diet (6). Others have found that higher insulin resistance, as measured by the quantitative insulin sensitivity check index, corresponded to less hippocampal and prefrontal gray matter in adolescents and young adults (18). Presently, there is a lack of longitudinal work that clarifies the relationship between insulin resistance, brain volume, and cognition (19).

In this study, we used voxel-wise methods (20) to test the relationship between insulin resistance and regional gray matter volume at baseline and follow-up roughly 4 years later in a middle-aged sample of healthy adults. Insulin resistance was indexed by the homeostasis model assessment of insulin resistance (HOMA-IR) (21). Regional gray matter volume was indexed by baseline and follow-up T1-weighted magnetic resonance imaging (MRI). We hypothesized that higher HOMA-IR would be associated with less gray matter at baseline and progressive atrophy in brain regions that are sensitive to insulin-signaling dynamics and affected by Alzheimer disease. Some of these regions include the anterior medial temporal lobe, prefrontal gyri, cingulate cortices, precuneus, and insula (2,8,10,14,17). Additionally, we tested for an interaction between HOMA-IR and poor glucoregulatory control, defined as a participant having prediabetes or type 2 diabetes. Higher HOMA-IR among participants with these conditions, but not in normoglycemic control subjects, corresponded to less glucose uptake in brain regions affected by early Alzheimer disease (22). By contrast, higher HOMA-IR showed no unique associations with regional gray matter in aged adults with type 1 or type 2 diabetes (16).

A final aim was to use a noncircular, independent region-of-interest approach (23) to examine whether insulin resistance, mean gray matter volume in hippocampus and parahippocampus, and Rey Auditory Verbal Learning Test (RAVLT) performance were interrelated at baseline and follow-up. Our primary interest was to see whether less gray matter mediated lower RAVLT scores specifically through the predicted influence of insulin resistance, suggesting that insulin resistance could be one factor that induces brain

atrophy and consequently affects cognition. Impaired episodic memory retrieval is a hallmark of early Alzheimer disease (24), and both deficits in glucose regulation and lower hippocampal volume are associated with episodic memory decline in healthy middle-aged to older adults (3). The region of interest was chosen because anterior medial temporal areas, particularly entorhinal cortex and hippocampus, are sensitive to early Alzheimer disease (25,26). By examining a unique cohort, the Wisconsin Registry for Alzheimer's Prevention (WRAP) (27), we were able to ascertain the relationship of insulin resistance with brain volume and cognition while controlling for known Alzheimer disease risk factors such as parental family history of Alzheimer disease and apolipoprotein (APO)E genotype (28,29).

RESEARCH DESIGN AND
METHODS—Three hundred and seventy-two late middle–aged, asymptomatic participants (mean ± SD age 57.66 ± 7.52 years) were assessed. A consecutive subset of participants ($n = 121$) had a follow-up volumetric brain scan roughly 4 years after the baseline scan (mean time elapsed 3.79 ± 0.99 years). Demographic information is available in Table 1. Participants are part of an ongoing study for WRAP, which investigates the contribution of Alzheimer disease risk factors to changes

in cognition and brain over time (27). The WRAP cohort consists of persons who were ~40–65 years of age at baseline. Participants are distinguished by either *1*) having no family history of Alzheimer disease or *2*) having a mother and/or father with probable Alzheimer disease based on clinical examination or medical record review using National Institutes of Health criteria (30) or with autopsy confirmation of Alzheimer disease. Collected data included basal glucose and insulin, APOE genotype, family history, and RAVLT scores. Exclusion criteria included contraindication to MRI scanning, abnormal MRI artifacts or excessive motion of >3 mm, and diagnosis of dementia, stroke, or multiple sclerosis. This study was conducted with prior written and informed consent of the participants and approved by the University of Wisconsin-Madison institutional review board.

Insulin resistance, BMI, and diabetes status
Basal glucose and basal insulin were collected in participants fasted for at least 12 h near the time of the MRI scan. Insulin resistance was determined by calculating HOMA-IR, which strongly correlates with the euglycemic-hyperinsulinemic clamp method of determining insulin-signaling efficacy (21). HOMA-IR was calculated using the following equation:

Table 1—*Demographic, neuropsychological, genetic, and glucoregulatory data*

	Baseline	Follow-up
n	372	121
Sex	102 male, 270 female	45 male, 76 female
Age (years)	57.67 ± 6.48	60.71 ± 6.18
Education (years)	16.39 ± 3.47	16.43 ± 3.13
BMI (kg/m^2)	27.68 ± 5.22	27.39 ± 4.77
HOMA-IR	2.15 ± 2.23	2.10 ± 1.75
Diabetes status		
Normoglycemic (<100 mg/dL)	270	83
Prediabetes (<126 mg/dL)	95	35
Type 2 diabetes (≥126 mg/dL)	7	3
Family history status		
Negative	92	37
Positive	280	84
APOE genotype		
Non-APOE4	246	75
APOE ε4 (hetero- or homozygous)	135	46
Baseline RAVLT		
Trials 1–5 (total)	51.82 ± 8.29	51.87 ± 8.04
Trial 6: short delay	10.80 ± 2.70	10.53 ± 2.46
Trial 7: extended delay	10.60 ± 3.09	10.43 ± 2.81

Data are *n* or means ± SD. Education was determined at the onset of WRAP.

$$\frac{\text{Basal glucose (mg/dL)} \times \text{basal insulin (}\mu\text{U/mL})}{405}.$$

BMI was used as a covariate because obesity can adversely affect the brain through nonmetabolic mechanisms such as inflammation (31). The presence of type 2 diabetes or prediabetes was determined from fasted blood glucose using current guidelines from the American Diabetes Association summarized in Table 1. Given that some participants classified as having prediabetes may have lower blood glucose because of type 2 diabetes medication, and the small number of participants with type 2 diabetes, both groups were combined for subsequent analysis.

APOE genotyping
Determination of APOE genotype has previously been described (28). In brief, DNA was isolated and nested PCR amplification used to analyze two single nucleotide polymorphisms (SNPs) of interest: rs429358 and rs7412. Automated sequence analysis (Agent, Paracel; Celera Genomics, Alameda, CA) was used to determine the nucleotide sequence position and allele for each SNP. APOE alleles were classified as having an ε2, ε3, or ε4 isoform. Participants were distinguished using a binary categorical variable, where one could be classified as "non-APOE4" (no ε4 allele present) or "APOE" (one or two ε4 alleles present).

RAVLT
Each participant was tested on the RAVLT (32) as previously described (27). This 15-item verbal list-learning test is an important predictor of conversion to Alzheimer disease (33). We examined the total score of encoding trials 1–5, the short delay free recall trial, and the long-delay free recall trial.

MRI acquisition
As previously described (28), a T1-weighted three-dimensional fast spoiled gradient-echo scan was acquired across three similar 3T General Electric (Waukesha, WI) scanners to assess regional brain volume. Among a subset of 121 participants, a follow-up scan was collected ~4 years later on a single scanner. Scanner type was included as a covariate in the baseline statistical analyses. A radiologist inspected anatomical images for potential abnormalities that would preclude their use in voxel-wise analyses.

MRI preprocessing
Cross-sectional. T1-weighted images acquired at baseline were first processed using a unified segmentation routine (34) in the package Statistical Parametric Mapping 8 (SPM8; http://www.fil.ion.ucl.ac.uk/spm/software/spm8/). In brief, for a given brain, the SPM8 "new segmentation" toolbox simultaneously *1*) uses affine normalization and nonlinear deformation warping to overlap the baseline brain image with the Montreal Neurologic Institute (MNI) neural atlas space and *2*) uses prior probability maps to parse the brain into spatially distinct tissue classes, including gray matter, white matter, cerebrospinal fluid, bone, fat, and unclassified tissue. This process automatically minimizes intensity nonuniformities. Tissue class maps were modulated to preserve individual variations in brain volume. An 8-mm Gaussian smoothing kernel was applied to maximize the signal-to-noise ratio, correct for minor alignment errors, and facilitate comparison across subjects.
Longitudinal. To assess atrophy specific to gray matter volume, we modulated the baseline scan by the degree of volumetric change between it and a follow-up MRI using a modified tensor-based morphometry procedure (35). A schematic summary of the procedure is provided in Supplementary Fig. 1. First, follow-up images were linearly coregistered to baseline images for each participant without reslicing, followed by high-dimensional warping to maximize spatial conformity via a nonlinear deformation field. This step produced a three-dimensional map of Jacobian determinants for each participant, which represents the degree of contraction or expansion required to transform a given voxel from the follow-up scan to the same voxel space in the baseline scan. This Jacobian map was aligned to MNI space using the transformational matrix from the segmentation step described above. This MNI-normalized Jacobian map was then multiplied by the baseline gray matter image in MNI space for each participant. The resultant image represents regional gray matter at baseline modulated by change over time, which is an index of progressive brain atrophy.
Region of interest. To confirm and extend voxel-wise analyses, we used an independent region-of-interest approach to avoid circular analysis (23). Mean gray matter volume in a single region of interest spanning both hippocampus and parahippocampus was extracted from baseline and follow-up scans. Regions were specified using the Wake Forest PickAtlas in SPM8 (http://fmri.wfubmc.edu/software/PickAtlas). These estimates were correlated with HOMA-IR and RAVLT at baseline and follow-up.

Voxel-wise statistics
For voxel-wise analyses, multiple regression models were tested in SPM8 using a single design matrix. The predictor of interest was either HOMA-IR or the HOMA-IR by diabetes status interaction. The dependent variable was the baseline gray matter image for cross-sectional analyses, while Jacobian-adjusted gray matter images were used for longitudinal analyses. Covariates included age, sex, family history, APOE status, MRI scanner, the number of days elapsed between the scan and blood sample collection, BMI, and diabetes status (normoglycemic vs. pre- and type 2 diabetes). Global gray matter was used as an additional covariate at baseline to adjust for brain size. This covariate was not necessary in longitudinal analyses because a global deformation field already removed variance related to differences in total brain size.

The probability values for voxel and cluster thresholds were 0.005 (uncorrected) and 0.05 (corrected), respectively. Results were considered significant at the cluster level. We minimized type 1 error by first using a threshold of 0.2 to ensure that voxels with <20% likelihood of being gray matter were not analyzed. Next, Monte Carlo simulations in AlphaSim (http://afni.nimh.nih.gov/afni/doc/manual/alphasim) were used to estimate the required number of contiguous voxels needed for a cluster to occur at $P < 0.05$. To ensure that this estimate was not biased by nonstationarity (36), we used SPM8 to render volumetric images uniformly smooth.

Nonvoxel statistics
All other analyses were conducted in SPSS 19.0 (SPSS, Chicago, IL). α was set at 0.05. A classic mediation approach (37) was used to examine whether less gray matter in the hippocampal and parahippocampal region of interest, either at baseline or with progressive atrophy, mediated worse RAVLT performance due to higher HOMA-IR values. Thus, partial correlations were conducted using the same covariates as the voxel-wise analyses. This correlational approach is comparable with previous reports that assessed interrelationships between

insulin resistance, gray matter volume, and cognition (3). Path analysis or other advanced techniques were not used because of insufficient sample size in the longitudinal analysis. Logarithmic or square root transformations were used to improve data normality or variance uniformity (i.e., homoscedasticity).

RESULTS

Participant information

Demographics, genotype data, laboratory measures from blood, and RAVLT scores for both baseline and follow-up visits are listed in Table 1.

Voxel-wise analyses

HOMA-IR. No significant effect of scanner type was found. Across all 372 participants, higher HOMA-IR was significantly associated with less gray matter at baseline in several regions implicated in early Alzheimer disease. For instance, two bilateral clusters were found in medial temporal lobe, which included anterior hippocampus and parahippocampus (Fig. 1 and Supplementary Table 1). The clusters also included middle and superior temporal pole, insula, and prefrontal gyri and most of cingulate gyrus, although little coverage was noted in posterior cingulate cortex. Additional subcortical structures included the amygdala, striatum, and pallidum. In the posterior and dorsal portions of brain, higher HOMA-IR predicted lower gray matter in inferior and superior parietal gyri, precuneus, paracentral lobule, occipital lobe, and anterior cerebellum.

A subsequent analysis of 121 individuals examined to what degree higher HOMA-IR predicted progressive atrophy in gray matter between the baseline and follow-up MRI scans. A representative voxel in occipital lobe (Fig. 2) indicates that, compared with the cross-sectional analysis, higher insulin resistance predicted less gray matter to a stronger extent. Akin to baseline results, this association produced large clusters that encompassed parietal gyri and precuneus and much of cingulate cortex (Supplementary Table 2). Rostral areas included anterior hippocampus, parahippocampus, temporal pole, and prefrontal gyri. Edge effects were not responsible for any clusters generated.

HOMA-IR and diabetes status. It was worthwhile to examine whether there were unique associations between insulin resistance and gray matter volume in participants with prediabetes or type 2 diabetes. Initially, a HOMA-IR × diabetes status interaction produced no significant clusters. For exploratory purposes, we also separately regressed HOMA-IR onto baseline gray matter volume for a single group of participants with prediabetes ($n = 95$) and type 2 diabetes ($n = 7$). Only one cluster attained significance in left fusiform gyrus (maximum at -34, -36, and -17, $t = 3.90$, number of voxels = 391). For longitudinal data, a HOMA-IR × diabetes status interaction produced no significant clusters among 84 adults with normal glycemic values versus 38 persons with prediabetes ($n = 35$) or type 2 diabetes ($n = 3$). A separate analysis of individuals with prediabetes and type 2 diabetes was not conducted because of small sample size.

HOMA-IR, cognition, and region-of-interest analyses

Partial correlation analysis was used to assess interrelationships between insulin resistance, gray matter in medial temporal lobe, and RAVLT scores. Our primary interest was to examine whether higher insulin resistance would significantly predict lower gray matter, where that relationship in turn would mediate lower RAVLT scores. Change in cognition over time was calculated by taking RAVLT scores at follow-up and subtracting out the baseline RAVLT values. Covariates were the same as the voxel-wise analyses and included age, sex, family history, APOE status, MRI scanner, the number of days between the scan and when blood samples were obtained, BMI, and type 2 diabetes status, as well as global gray matter for baseline analyses. (See RESEARCH DESIGN AND METHODS.)

For baseline data, higher HOMA-IR was modestly related to lower mean hippocampal and parahippocampal volume (partial $R^2 = 0.01$, $P \leq 0.05$). Neither gray matter nor HOMA-IR was correlated with baseline RAVLT trial scores (data not shown). These results suggest that insulin resistance did not influence cognition directly or through associations with gray matter at baseline.

For longitudinal data, higher HOMA-IR predicted progressive atrophy in the gray matter region of interest (partial $R^2 = 0.025$, $P \leq 0.05$). HOMA-IR itself was significantly correlated with worse performance over time in encoding trials 1–5 (partial $R^2 = 0.027$, $P \leq 0.05$) but not the short delay (partial $R^2 = 4 \times 10^{-6}$, N.S.) or extended delay (partial $R^2 = 8 \times 10^{-4}$,
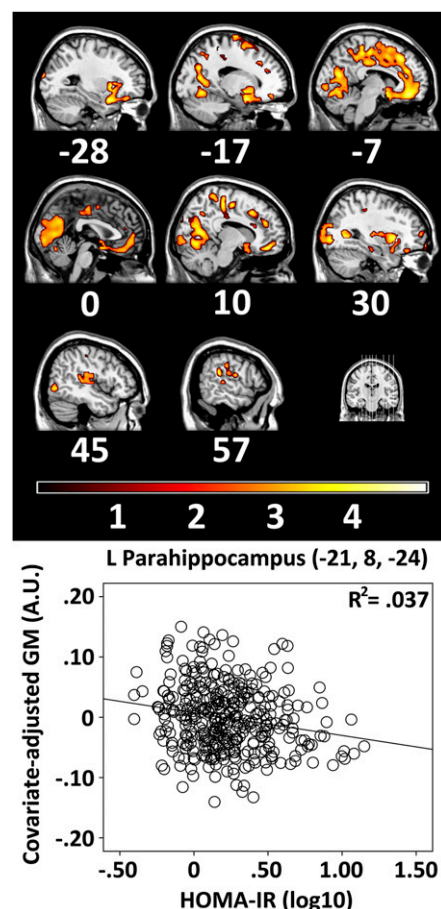

Figure 1—*The relationship between higher HOMA-IR and lower regional gray matter (GM) volume for baseline images among 372 participants. Coordinates correspond to sagittal cross-sections in MNI space. An orthogonal coronal image illustrates the location of these cross-sections in the brain. The result color map and color bar represent* t *values. A representative voxel in parahippocampus depicts the association. Brains are oriented in neurologic space. A.U., arbitrary units. L, left. (A high-quality digital representation of this figure is available in the online issue.)*

N.S.) trials (Supplementary Fig. 2A). As mentioned above and depicted in Supplementary Fig. 2B, higher HOMA-IR also predicted progressive atrophy in the region encompassing hippocampus and parahippocampus. Finally, gray matter atrophy was related to lower RAVLT scores over time in the short delay (partial $R^2 = 0.048$, $P \leq 0.05$) and extended delay (partial $R^2 = 0.050$, $P \leq 0.05$) tasks but not encoding trials 1–5 initially (partial $R^2 = 0.016$, $P = 0.100$). However, when covarying out the effect of HOMA-IR, progressive atrophy did predict worse RAVLT performance in trials 1–5 as shown in Supplementary Fig. 2C (partial $R^2 = 0.027$,
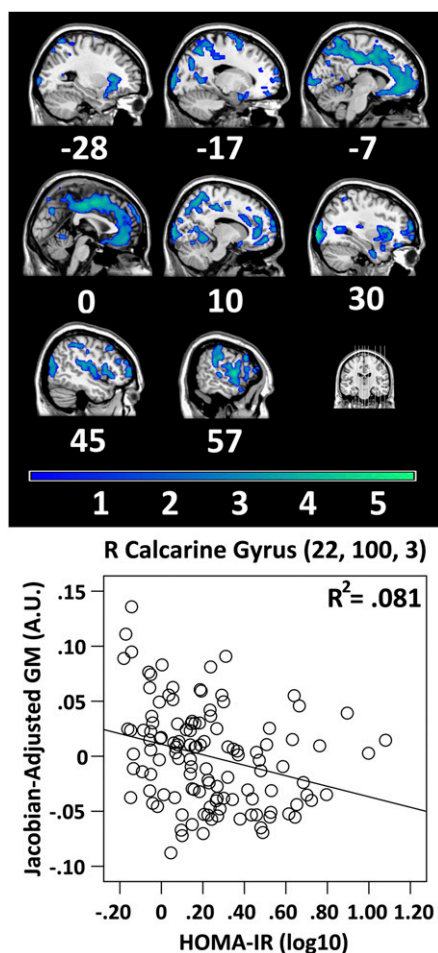
Figure 2—*The association between higher HOMA-IR and atrophy in regional gray matter (GM) volume over ~4 years for 121 participants with longitudinal data. Coordinates correspond to sagittal cross-sections in MNI space. An orthogonal coronal image illustrates the location of these cross-sections in the brain. The color map and bar represent t values. A representative voxel in calcarine gyrus depicts the association. Brains are oriented in neurologic space. A.U., arbitrary units. R, right. (A high-quality digital representation of this figure is available in the online issue.)*

$P \leq 0.05$). While this result is atypical for classical mediation (37), it nonetheless suggests that higher HOMA-IR is associated with lower medial temporal lobe volume, a relationship that may mediate worse RAVLT encoding performance.

CONCLUSIONS—In this study of late middle–aged, asymptomatic adults in the WRAP cohort, separate voxel-wise and region-of-interest results indicated that HOMA-IR was significantly associated across 372 participants with less baseline gray matter volume in brain areas affected by early Alzheimer disease. These

findings were stronger when examining progressive gray matter atrophy over a roughly 4-year period in a consecutive subset of 121 people. There were also small correlations between insulin resistance, gray matter in a region of anterior medial temporal lobe, and the RAVLT. While prediabetes or type 2 diabetes based on fasting glucose levels did not significantly influence these relationships, there were few participants with type 2 diabetes. Nonetheless, Benedict et al. (16) indicated that higher HOMA-IR was not uniquely associated with gray matter volume in geriatric adults with type 1 or 2 diabetes versus the full cohort. Given the potent influence that insulin resistance can have on glucose uptake when prediabetes or type 2 diabetes is present (22), additional longitudinal studies are needed that incorporate more late middle–aged people with glucoregulatory dysfunction.

For voxel-wise analyses, several of the brain regions evincing insulin resistance–related atrophy were similar to those showing change in early Alzheimer disease. Most studies to date have found that measures of insulin resistance correspond to lower hippocampal volume either cross-sectionally (3,13) or longitudinally (14). In our sample, this association was predominantly found in anterior hippocampus abutting the amygdala and parahippocampus. This result is important because morphological changes in entorhinal cortex and anterior hippocampus, particularly the cornu ammonis fields, are sensitive to mild cognitive impairment and early Alzheimer disease relative to normative aging (25,26). Insulin resistance may affect more posterior portions of hippocampus in at-risk participants as they become older. However, higher insulin resistance in a cross-section of healthy aged adults did not correspond to lower hippocampal volume as assessed by MRI (16).

Insulin resistance also predicted lower baseline gray matter and more volumetric atrophy over time along a neuroaxis spanning from subgenual cingulate to orbitofrontal and dorsolateral cortices and then caudally to precuneus and superior parietal areas. Annual atrophy rates in very early mild cognitive impairment up to early Alzheimer disease illustrate a similar pattern (38). Higher insulin levels, typical of insulin resistance, have also been paradoxically associated with ameliorative rather than pathological changes in cingulate cortex in early

Alzheimer disease (17). Curiously, however, HOMA-IR in this study was not associated with gray matter in most of the posterior cingulate gyrus. HOMA-IR dysregulates basal and task-based glucose uptake in this area among aged participants with prediabetes or type 2 diabetes (22). Although insulin resistance in late middle age may not induce pronounced atrophy via hypometabolism in posterior cingulate cortex, energy dysregulation in this area is nonetheless an important factor in Alzheimer disease (39).

The associations between HOMA-IR, an independently chosen region of interest, including hippocampus and parahippocampus, and RAVLT scores were modest but consistent. HOMA-IR predicted less gray matter in this region at baseline, as well as increased progressive atrophy over the course of ~4 years. These regions are some of the first areas to show atrophy in mild cognitive impairment or Alzheimer disease (38,40). Baseline volume in medial temporal lobe or HOMA-IR did not predict deficits in memory at baseline. By contrast, progressive atrophy in hippocampus and parahippocampus appeared to mediate lower encoding trial performance due to higher HOMA-IR. Although RAVLT delayed recall is an important predictor of conversion from the asymptomatic phase to mild cognitive impairment or directly to Alzheimer disease (33), deficits in encoding are also characteristic of the disease. It is therefore of interest to continue examining this cohort to see whether these relationships remain and possibly become stronger over time as individuals in the WRAP cohort begin to show cognitive decline.

There are several limitations that should be addressed. Although several participants had prediabetes, there were few cases of type 2 diabetes. This deficit limits the ability to compare current results with other studies with a proportionally larger glucoregulatory disease cohort (22). Furthermore, data were not available to ascertain whether duration of prediabetes or type 2 diabetes might have affected analyses pertaining to hyperglycemia. Although BMI was used as an index of obesity, waist circumference would have been a more sensitive index. While HOMA-IR, medial temporal gray matter atrophy, and RAVLT scores were significantly associated with one another, these correlations were small. In middle-aged participants, however, there is minimal atrophy and subtle variation in cognition relative to mild cognitive

impairment or Alzheimer disease in aged individuals. It was also beyond the scope of this report to investigate biological mechanisms that could underlie the association between insulin resistance, brain, and cognition, such as proinflammatory cytokine expression, mitochondrial dysfunction, microvascular damage, or deficits in glucose uptake and amyloid clearance. Such analyses require future studies to focus on those physiological parameters. Finally, despite associations between HOMA-IR and gray matter volume at baseline and follow-up, it is not appropriate to make direct causal inferences based on these findings.

In conclusion, our study suggests that insulin resistance may be a risk factor for the development of atrophy and cognitive deficits reminiscent of Alzheimer disease. Among late middle–aged participants, HOMA-IR predicted gray matter atrophy in cingulate cortices, medial temporal lobe, prefrontal gyri, and other regions that are sensitive to Alzheimer disease pathogenesis. HOMA-IR was also related to worse RAVLT encoding performance. Progressive medial temporal atrophy but not baseline gray matter also predicted significant decreases in RAVLT scores. Finally, HOMA-IR predicted medial temporal atrophy, which in turn mediated lower RAVLT encoding performance. It will be worthwhile to extend these results by examining whether HOMA-IR is related to lower glucose uptake, increased amyloid β binding, or other factors that precipitate neural atrophy and disease onset.

References

1. de la Monte SM, Wands JR. Review of insulin and insulin-like growth factor expression, signaling, and malfunction in the central nervous system: relevance to Alzheimer's disease. J Alzheimers Dis 2005;7:45–61
2. Craft S, Watson GS. Insulin and neurodegenerative disease: shared and specific mechanisms. Lancet Neurol 2004;3:169–178
3. Convit A, Wolf OT, Tarshish C, de Leon MJ. Reduced glucose tolerance is associated with poor memory performance and hippocampal atrophy among normal elderly. Proc Natl Acad Sci USA 2003;100:2019–2022
4. Schrijvers EM, Witteman JC, Sijbrands EJ, Hofman A, Koudstaal PJ, Breteler MM. Insulin metabolism and the risk of Alzheimer disease: the Rotterdam Study. Neurology 2010;75:1982–1987
5. Blalock EM, Grondin R, Chen KC, et al. Aging-related gene expression in hippocampus proper compared with dentate gyrus is selectively associated with metabolic syndrome variables in rhesus monkeys. J Neurosci 2010;30:6058–6071
6. Willette AA, Bendlin BB, Colman RJ, et al. Calorie restriction reduces the influence of glucoregulatory dysfunction on regional brain volume in aged rhesus monkeys. Diabetes 2012;61:1036–1042
7. Cersosimo E, DeFronzo RA. Insulin resistance and endothelial dysfunction: the road map to cardiovascular diseases. Diabetes Metab Res Rev 2006;22:423–436
8. Henneberg N, Hoyer S. Desensitization of the neuronal insulin receptor: a new approach in the etiopathogenesis of late-onset sporadic dementia of the Alzheimer type (SDAT)? Arch Gerontol Geriatr 1995;21:63–74
9. Zhao WQ, Chen H, Quon MJ, Alkon DL. Insulin and the insulin receptor in experimental models of learning and memory. Eur J Pharmacol 2004;490:71–81
10. Gasparini L, Gouras GK, Wang R, et al. Stimulation of beta-amyloid precursor protein trafficking by insulin reduces intraneuronal beta-amyloid and requires mitogen-activated protein kinase signaling. J Neurosci 2001;21:2561–2570
11. Zhao WQ, Lacor PN, Chen H, et al. Insulin receptor dysfunction impairs cellular clearance of neurotoxic oligomeric abeta. J Biol Chem 2009;284:18742–18753
12. Planel E, Tatebayashi Y, Miyasaka T, et al. Insulin dysfunction induces in vivo tau hyperphosphorylation through distinct mechanisms. J Neurosci 2007;27:13635–13648
13. Rasgon NL, Kenna HA, Wroolie TE, et al. Insulin resistance and hippocampal volume in women at risk for Alzheimer's disease. Neurobiol Aging 2011;32:1942–1948
14. Raji CA, Ho AJ, Parikshak NN, et al. Brain structure and obesity. Hum Brain Mapp 2010;31:353–364
15. Tan ZS, Beiser AS, Fox CS, et al. Association of metabolic dysregulation with volumetric brain magnetic resonance imaging and cognitive markers of subclinical brain aging in middle-aged adults: the Framingham Offspring Study. Diabetes Care 2011;34:1766–1770
16. Benedict C, Brooks SJ, Kullberg J, et al. Impaired insulin sensitivity as indexed by the HOMA score is associated with deficits in verbal fluency and temporal lobe gray matter volume in the elderly. Diabetes Care 2012;35:488–494
17. Burns JM, Honea RA, Vidoni ED, Hutfles LJ, Brooks WM, Swerdlow RH. Insulin is differentially related to cognitive decline and atrophy in Alzheimer's disease and aging. Biochim Biophys Acta 2012;1822:333–339
18. Ursache A, Wedin W, Tirsi A, Convit A. Preliminary evidence for obesity and elevations in fasting insulin mediating associations between cortisol awakening response and hippocampal volumes and frontal atrophy. Psychoneuroendocrinology 2012;37:1270–1276
19. Raz N. Diabetes: brain, mind, insulin-what is normal and do we need to know? Nat Rev Endocrinol 2011;7:636–637
20. Ashburner J, Friston KJ. Voxel-based morphometry—the methods. Neuroimage 2000;11:805–821
21. Matthews DR, Hosker JP, Rudenski AS, Naylor BA, Treacher DF, Turner RC. Homeostasis model assessment: insulin resistance and beta-cell function from fasting plasma glucose and insulin concentrations in man. Diabetologia 1985;28:412–419
22. Baker LD, Cross DJ, Minoshima S, Belongia D, Watson GS, Craft S. Insulin resistance and Alzheimer-like reductions

in regional cerebral glucose metabolism for cognitively normal adults with prediabetes or early type 2 diabetes. Arch Neurol 2011;68:51–57

23. Kriegeskorte N, Lindquist MA, Nichols TE, Poldrack RA, Vul E. Everything you never wanted to know about circular analysis, but were afraid to ask. J Cereb Blood Flow Metab 2010;30:1551–1557

24. Mesulam M. *Principles of Behavior and Cognitive Neurology*. Oxford, Oxford University Press, 2000

25. Jack CR Jr, Petersen RC, Xu YC, et al. Prediction of AD with MRI-based hippocampal volume in mild cognitive impairment. Neurology 1999;52:1397–1403

26. Good CD, Johnsrude IS, Ashburner J, Henson RN, Friston KJ, Frackowiak RS. A voxel-based morphometric study of ageing in 465 normal adult human brains. Neuroimage 2001;14:21–36

27. Sager MA, Hermann B, La Rue A. Middle-aged children of persons with Alzheimer's disease: APOE genotypes and cognitive function in the Wisconsin Registry for Alzheimer's Prevention. J Geriatr Psychiatry Neurol 2005;18:245–249

28. Johnson SC, La Rue A, Hermann BP, et al. The effect of TOMM40 poly-T length on gray matter volume and cognition in middle-aged persons with APOE $\varepsilon 3/\varepsilon 3$ genotype. Alzheimers Dement 2011;7:456–465

29. Bendlin BB, Ries ML, Canu E, et al. White matter is altered with parental family history of Alzheimer's disease. Alzheimers Dement 2010;6:394–403

30. McKhann G, Drachman D, Folstein M, Katzman R, Price D, Stadlan EM. Clinical diagnosis of Alzheimer's disease: report of the NINCDS-ADRDA Work Group under the auspices of Department of Health and Human Services Task Force on Alzheimer's Disease. Neurology 1984;34:939–944

31. Haroon E, Raison CL, Miller AH. Psycho-neuroimmunology meets neuropsychopharmacology: translational implications of the impact of inflammation on behavior. Neuropsychopharmacology 2012;37:137–162

32. Spreen O, Strauss E. *A Compendium of Neuropsychological Tests: Administration, Norms, and Commentary*. 2nd ed. New York, Oxford University Press, 1998

33. Gomar JJ, Bobes-Bascaran MT, Conejero-Goldberg C, Davies P, Goldberg TE; Alzheimer's Disease Neuroimaging Initiative. Utility of combinations of biomarkers, cognitive markers, and risk factors to predict conversion from mild cognitive impairment to Alzheimer disease in patients in the Alzheimer's disease neuroimaging initiative. Arch Gen Psychiatry 2011;68:961–969

34. Ashburner J, Friston KJ. Unified segmentation. Neuroimage 2005;26:839–851

35. Kipps CM, Duggins AJ, Mahant N, Gomes L, Ashburner J, McCusker EA. Progression of structural neuropathology in preclinical Huntington's disease: a tensor based morphometry study. J Neurol Neurosurg Psychiatry 2005;76:650–655

36. Hayasaka S, Phan KL, Liberzon I, Worsley KJ, Nichols TE. Nonstationary cluster-size inference with random field and permutation methods. Neuroimage 2004;22:676–687

37. Baron RM, Kenny DA. The moderator-mediator variable distinction in social psychological research: conceptual, strategic, and statistical considerations. J Pers Soc Psychol 1986;51:1173–1182

38. McDonald CR, McEvoy LK, Gharapetian L, et al.; Alzheimer's Disease Neuroimaging Initiative. Regional rates of neocortical atrophy from normal aging to early Alzheimer disease. Neurology 2009;73:457–465

39. Minoshima S, Giordani B, Berent S, Frey KA, Foster NL, Kuhl DE. Metabolic reduction in the posterior cingulate cortex in very early Alzheimer's disease. Ann Neurol 1997;42:85–94

40. Braak H, Thal DR, Ghebremedhin E, Del Tredici K. Stages of the pathologic process in Alzheimer disease: age categories from 1 to 100 years. J Neuropathol Exp Neurol 2011;70:960–969